JOURNAL OF GEOPHYSICAL RESEARCH, VOL. 107, NO. C12, 3226, doi:10.1029/2001JC001098, 2002

A dual-frequency approach for retrieving sea surface wind speed from TOPEX altimetry

Ge Chen
Ocean Remote Sensing Institute, Ocean University of China, Qingdao, China

Bertrand Chapron and Robert Ezraty
Département d'Océanographie Physique et Spatiale, Centre de Brest, IFREMER, Plouzané, France

Douglas Vandemark
Laboratory for Hydrospheric Processes, Wallops Flight Facility, NASA Goddard Space Flight Center, Wallops Island, Virginia, USA

Received 13 August 2001; revised 10 April 2002; accepted 24 April 2002; published 21 December 2002.

[1] More than a dozen of wind speed (U) algorithms have been proposed during the past 2 decades, as a result of a continuing effort to improve altimeter wind measurement. The progress in terms of accuracy, however, is seen to be rather slow. The reported root mean square (RMS) error of prevailing algorithms varies mostly between 1.6 and 2.0 m/s for the dominant wind regime. As far as the TOPEX altimeter is concerned, three measured quantities, namely, the radar cross sections from Ku and C band (σ_{Ku} and σ_C), as well as the significant wave height (H_s), have been used in previous algorithm developments, resulting in a variety of single-, dual-, and three-parameter model functions. On the basis of the finding of a banded dependency of the U–σ_{Ku} relationship on σ_C a new approach for retrieving altimeter wind speed, termed linear composite method (LCM), is proposed in this study. The LCM model function appears as a set of σ_C-dependent linear relations between U and σ_{Ku}. A unique advantage of this approach is that it allows the algorithm to be tuned or expanded for a given range of wind speed without affecting the rest. Over 1.7 million coincident TOPEX/NASA scatterometer (NSCAT) and TOPEX/QuikSCAT data covering a period of 2.5 years are used to adjust the model. Validation against extensive buoy measurements indicates that the LCM algorithm is almost unbiased and has an overall RMS error of 1.56 m/s, which is 12% lower compared to the algorithm in operational use [*Witter and Chelton*, 1991]. In addition, a small (2.5–6%, depending on the reference data set) but significant improvement is found for the LCM when compared to the most recent dual-parameter algorithm [*Gourrion et al.*, 2002]. *INDEX TERMS:* 4275 Oceanography: General: Remote sensing and electromagnetic processes (0689); 4504 Oceanography: Physical: Air/sea interactions (0312); 4506 Oceanography: Physical: Capillary waves; *KEYWORDS:* sea surface wind speed, retrieval, TOPEX, altimeter, dual frequency

Citation: Chen, G., B. Chapron, R. Ezraty, and D. Vandemark, A dual-frequency approach for retrieving sea surface wind speed from TOPEX altimetry, *J. Geophys. Res.*, *107*(C12), 3226, doi:10.1029/2001JC001098, 2002.

1. Introduction

[2] The development of altimeter wind speed measurement over the past twenty years is, to some extent, accompanied by an increasing number of variables in the algorithm. These variables include at least the radar cross sections at Ku and C bands (σ_{Ku} and σ_C), and the significant wave height (H_s). A general motivation behind is perhaps the anticipation that multiple parameters in the algorithm may bring additional or complementary information which can improve the accuracy of altimeter wind speed inversion. The algorithms proposed in 1980s and early 1990s are mostly single-parameter (σ_{Ku}) based [e.g., *Brown et al.*, 1981; *Witter and Chelton*, 1991]. Several dual-parameter (σ_{Ku} and H_s) model functions were developed around mid-1990s [e.g., *Glazman and Greysukh*, 1993; *Lefevre et al.*, 1994]. More recently, *Elfouhaily et al.* [1998] proposed an iterative scheme for altimeter wind speed estimation which involves three parameters (σ_{Ku}, σ_C and H_s). It is somewhat surprising that the progress made by incorporating additional variables in the algorithms is far from obvious for years, although this situation may start to change as a result of some very recent developments [*Gommenginger et al.*, 2002; *Gourrion et al.*, 2002].

[3] A detailed review and comparison of several single-parameter wind speed algorithms are given by *Lefevre et al.* [1994], and *Freilich and Challenor* [1994]. As expected, the

0148-0227/02/2001JC001098$09.00

Table 1. Some Details of the Collocation Data Set Used in the Development and Validation of the LCM Wind Speed Algorithm for TOPEX

Collocation Data set	TOPEX/NSCAT	TOPEX/QSCAT	TOPEX/Buoy	TOPEX/ECMWF
Duration	15 Sept 1996 to 30 June 1997	20 July 1999 to 19 March 2001	25 Sept. 1992 to 31 Dec. 1998	15 Sept. 1996 to 30 June 1997
Latitudinal coverage	66°S–66°N	66°S–66°N	17.2°–59.3°N	66°S–66°N
Number of data	97,613	1,639,075	4,512	97,613
Time window, hour	1.0	0.5	1.0	3.0
Space window, km	12	15	50	60–125

relative performance of these algorithms is wind speed dependent, none of them is seen to be absolutely superior to others. Meanwhile, a number of investigators have introduced significant wave height as a second parameter in their model functions. An obvious attraction in these efforts is that the altimeters provide simultaneous measurements of radar cross section and significant wave height at each nadir point. *Glazman and Greysukh* [1993] developed a set of wave age–based wind speed algorithms using Chebyshev polynomials. *Lefevre et al.* [1994] proposed a series of model functions in which the wind speed is expressed as a quadratic polynomial of σ_{Ku} and H_s. Both studies have reported marginal improvement of their dual-parameter wind speed estimates compared to single-parameter algorithms. Even this, however, is not free from controversy. As *Wu* [1999] pointed out, the variations of altimeter returns attributed to the influence of dominant ocean waves by *Glazman and Greysukh* [1993] appear to be provided, at least in part, by the systematic deviation in the algorithm of *Brown et al.* [1981]. In contrast, a recent attempt by *Gourrion et al.* [2002] provides new evidence that (σ_{Ku}, H_s) based dual-parameter algorithm is indeed able to produce encouraging results. In that study, the altimeter wind model was defined using a multilayer perceptron neural network with altimeter derived σ_{Ku} and H_s as inputs. A 10–15% reduction of RMS error was reported in comparison with existing altimeter wind algorithms.

[4] *Elfouhaily et al.* [1998] presented a theoretically based method for inferring wind speed from a combination of σ_{Ku}, σ_C and H_s measurements. The basis for this approach is that the difference between σ_C and σ_{Ku} is related to the spectrum of short gravity waves with wavelengths in the range responsible for the difference in the backscatter at the two frequencies. *Elfouhaily et al.* [1998] derived an analytical relationship between the surface friction velocity and the two radar cross section measurements based on a prescribed wave spectrum. The estimates of friction velocity were then transformed into the neutral stability wind speed at 10 m height using a sea state dependent drag law. Since the drag law also depends on wind speed, the wind speed must be inferred iteratively. From comparisons with collocated buoy data, *Elfouhaily et al.* [1998] showed that the accuracy of their wind speed estimates was somewhat better than the single-frequency-based algorithm.

[5] Given the sophisticated [e.g., *Elfouhaily et al.*, 1998] and sometimes controversial [e.g., *Glazman and Greysukh*, 1993] nature of existing multiparameter wind speed algorithms, it is not surprising to see that a single-parameter algorithm by *Witter and Chelton* [1991] is still chosen for operational use in all current altimeter missions. However, it is the authors' view that the potential of the dual-frequency approach in improving altimeter wind measurement has not yet been fully explored. In fact, this technique has been proved very successful in observing oceanic precipitation [e.g., *Chen et al.*, 1997; *Quartly et al.*, 1999]. In this study, based on the analysis of a large volume of coincident data from TOPEX altimeter, NASA scatterometer (NSCAT) and QuikSCAT (hereinafter abbreviated as QSCAT) scatterometer, as well as buoy and ECMWF winds, we are going to demonstrate that σ_C, as an additional parameter, is more effective and straightforward in altimeter wind speed retrieval compared to H_s (section 2). A fundamentally different approach is then proposed for the development of TOPEX wind speed algorithm, yielding a set of σ_{Ku}-dependent linear model functions indexed by σ_C (section 3). The new algorithm is compared extensively with previous algorithms using collocated buoy and ECMWF winds (section 4). Finally, conclusions and recommendations are presented with an emphasis on the perspective of realizing the full potential of altimeter wind observations (section 5).

2. Collocation Data Set: Illustrating Wind Speed Dependency on H_s and σ_C

[6] In order to produce statistically significant and geophysically reliable results, a comprehensive collocation data set, including measurements from TOPEX altimeter, NSCAT and QSCAT scatterometers, and global buoys, as well as ECMWF wind estimates, has been compiled. Details regarding this data set are given in Table 1. To ensure a high quality, long duration and sufficient spatial resolution, a combination of NSCAT and QSCAT measurements is chosen as training data in our algorithm development; While buoy measured and ECMWF predicted winds are used for validation and comparison purposes. Since there is evidence indicating that near-incidence scatterometer measurements might be impacted by sea state effect [*Queffeulou et al.*, 1999], the crossover points where the NSCAT midbeam antenna has an incidence angle less than 40 degrees are eliminated from our data set.

[7] The TOPEX/NSCAT collocation data set is first used to generate scatter diagrams of U (from NSCAT) versus σ_{Ku} (from TOPEX) with respect to H_s (from TOPEX) and σ_C (from TOPEX), as illustrated in Figures 1a and 1b, respectively. Apart from the basically inverse relationship between U and σ_{Ku}, the two diagrams present a view of the actual wind speed dependence on H_s and σ_C. It can be seen from Figure 1a that low H_s is generally associated with low wind speed, and vice versa. However, there is a considerable overlap in the dependency of the U–σ_{Ku} relationship on H_s, especially for high and low winds beyond 5–15 m/s. In contrast, the U–σ_{Ku} relation with respect to σ_C, characterized by a regularly banded structure, is surprisingly well defined for the whole range of wind speed, as shown in

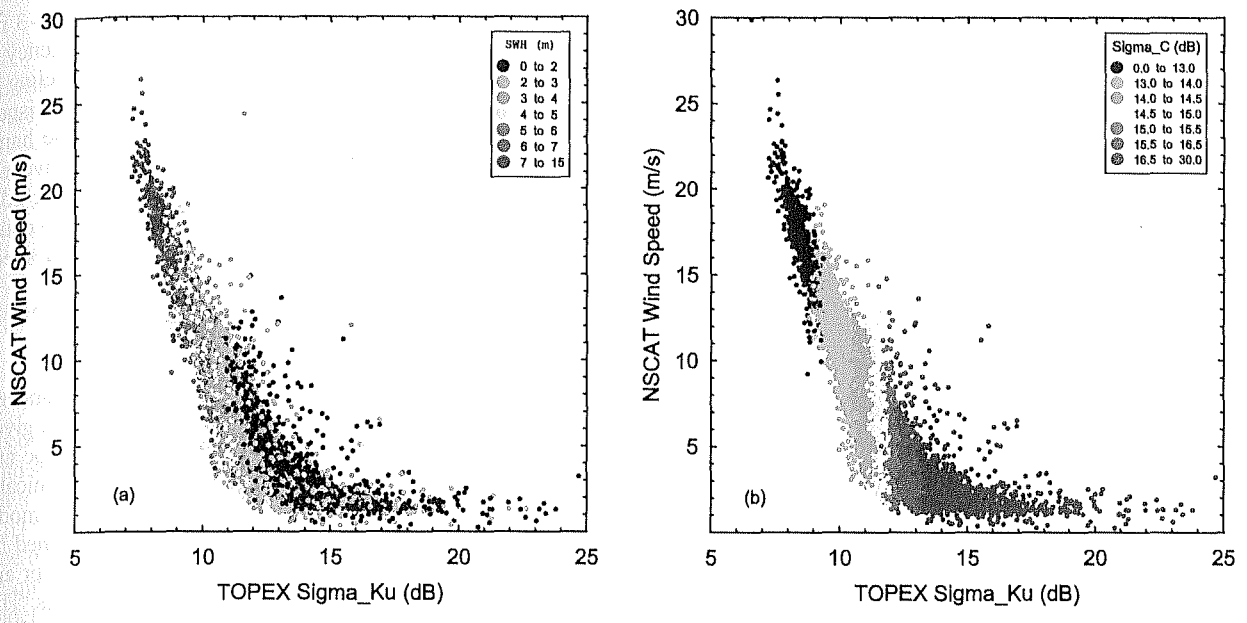

Figure 1. Scatter diagrams of collocated NSCAT wind speed and TOPEX radar cross section at Ku band. The color classification is based on (a) H_s and (b) σ_C.

Figure 1b. The relationship between U and σ_{Ku} is largely linear for a narrow band of σ_C, and there seems to be only a limited overlap for neighboring σ_{Ku}s. By comparing Figures 1a and 1b, it can be argued that σ_C might be a better surrogate than H_s as far as altimeter wind speed estimation is concerned. To support this argument, similar diagrams are generated using the TOPEX/Buoy collocation data set which spans a much longer time period (from 1992 to 1998), as shown in Figure 2. It is evident that the basic features identified in Figure 1 remain in Figure 2, except that the latter appears to be more scattered owing to the fact that the size of its spatial window is much larger (see Table 1).

[8] After confirming the observed difference in wind speed dependency on H_s and σ_C using an independent data set, we now return to Figure 1 for a different presentation. The TOPEX/NSCAT collocation data set used for plotting Figure 1 is divided into 10 sub-data sets according to H_s and σ_C, respectively. Information regarding the division is given in Table 2. For each sub-data set, the U–σ_{Ku} scatter points are binned according to σ_{Ku} with an interval of 0.1 dB, an

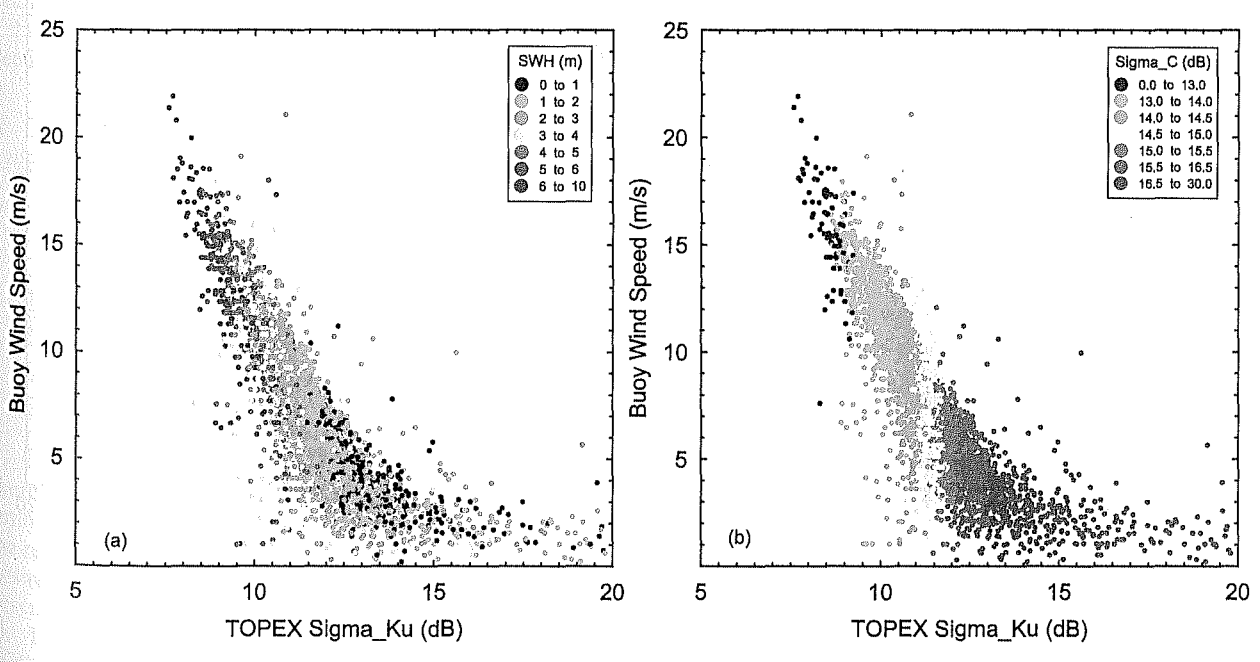

Figure 2. Same as Figure 1 but the TOPEX/Buoy collocation data set is used.

Table 2. Dividing Information of the Collocated TOPEX/NSCAT and TOPEX/QSCAT Sub-data Sets

Group Index (i)	H_s Band, m	σ_C Band, dB
1	9–15	0–12
2	8–9	12–13
3	7–8	13–14
4	6–7	14–15
5	5–6	15–16
6	4–5	16–17
7	3–4	17–18
8	2–3	18–19
9	1–2	19–20
A	0–1	20–30

average wind speed is then calculated for each bin, resulting in ten U–σ_{Ku} relations as shown in Figures 3a and 3b, respectively. Indeed, the way that wind speed depends on σ_C and H_s differs dramatically: The σ_C dependency appears to be clearly banded (Figure 3b), while the H_s dependency looks heavily overlapped (Figure 3a). The latter confirms an argument by *Queffeulou et al.* [1999] that significant wave height is an ambiguous wave field descriptor carrying a mixture of wind sea and swell information which can include very different degrees of sea state development. A closer inspection of Figures 3a and 3b allows at least two crucial differences to be identified. First, the U–σ_C dependency holds nicely for the whole range of wind speed; While the U–H_s dependency appears to be somewhat significant between 5–10 m/s, beyond which significant wave height carries little useful information for wind speed inversion. Second, for a given band of σ_C, the corresponding range of σ_{Ku} (and hence U) is relatively narrow, and the U–σ_{Ku} relationship is largely linear; While the dynamic range of σ_{Ku} for a given band of H_s is much wider, and the U–σ_{Ku} relationship for dominant significant wave heights (1–3 m) is basically nonlinear. Given the weak U–H_s dependency, it is easy to understand that low degree nonlinear modeling of U against σ_{Ku} is difficult to achieve the expected dispersions. These two substantial differences, on the one hand, explain, to a large extent, the reason why the effectiveness of some early H_s-based algorithms is marginal and controversial, on the other hand, indicate clearly that σ_C could be a better surrogate for improving altimeter wind speed estimates.

3. A Proposed New Approach

[9] Based on the analysis in section 2, the basic characteristics of Figure 3b can be understood as such: For a given σ_C, the U–σ_{Ku} relationship is largely linear, the slope and intercept of which vary continuously and monotonically with σ_C. It means that, if the altimeter wind speed model function (i.e., the slope and intercept) can be determined for a series of well distributed σ_Cs, the U–σ_{Ku} relation for any σ_C can then be obtained through linear interpolations. This forms the basic idea of the proposed scheme, termed "linear composite method" (or LCM for simplicity), for TOPEX wind speed derivation.

[10] Suppose the TOPEX wind speed model function is known at n different σ_C^is as,

$$U_T(\sigma_C^i) = a_i(\sigma_C^i)\sigma_{Ku} + b_i(\sigma_C^i) \quad (i = 1, 2, \cdots, n) \qquad (1)$$

where U_T is the TOPEX derived wind speed, a_i and b_i are model coefficients, and n is properly chosen to ensure a full coverage of the wind speed dynamic range with reasonable resolution. The U_T–σ_{Ku} relation at an arbitrary C band radar cross section, σ_C^x, can be expressed as

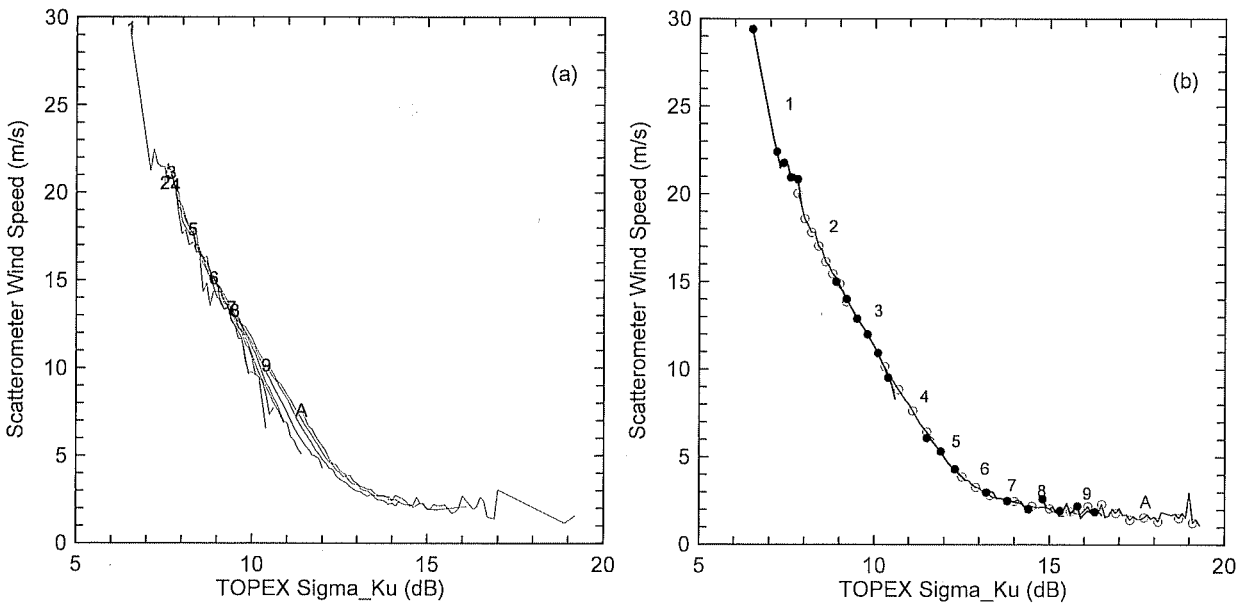

Figure 3. Binned averages of the classified scatter diagrams in Figure 1 (see Table 2 for the classifications). The resulting curve of each sub–data set is depicted (a) with the group index at its starting point and (b) with an alternating thick line with solid circles and thin line with open circles. The numbers over the curves of Figure 3b correspond to the group index in Table 2.

$$U_T(\sigma_C^x) = a_x(\sigma_C^x)\sigma_{Ku} + b_x(\sigma_C^x) \quad (1 \le x \le n) \tag{2}$$

We assume, without losing generality, that $j \le x \le j+1$, where $j = 1, 2, \ldots, n-1$. a_x and b_x can then be determined by

$$a_x(\sigma_C^x) = a_j(\sigma_C^j) + \left[a_{j+1}\left(\sigma_C^{j+1}\right) - a_j(\sigma_C^j)\right] \times \frac{(\sigma_C^x - \sigma_C^j)}{\left(\sigma_C^{j+1} - \sigma_C^j\right)} \tag{3a}$$

$$b_x(\sigma_C^x) = b_j(\sigma_C^j) + \left[b_{j+1}\left(\sigma_C^{j+1}\right) - b_j(\sigma_C^j)\right] \times \frac{(\sigma_C^x - \sigma_C^j)}{\left(\sigma_C^{j+1} - \sigma_C^j\right)} \tag{3b}$$

It is obvious that, once a_i and b_i in Equation (1) are available, wind speed can be estimated with any TOPEX measured σ_{Ku} and σ_C.

[11] Determination of a_i and b_i is crucial, as the performance of the proposed scheme will, to a large extent, rely on the quality of these coefficients. Like most of the empirical model functions, a_i and b_i will be determined via a least squares approach using a collocation data set. Following a thorough analysis and comparison, it is decided to use NSCAT and QSCAT data for modeling, while buoy and ECMWF data for validation. NSCAT is chosen because the instrument provided wind measurements with the highest spatial resolution and broadest coverage of any spaceborne scatterometer flown to date, and more importantly, its unprecedented accuracy of 1.3 m/s [*Freilich and Dunbar*, 1999] is approaching buoy measurements on a global scale. This is particularly attractive for regions where buoy data are not available. The addition of QSCAT data is to expand the collocation duration from 10 months to 2.5 years, which will greatly enhance the statistical significance.

[12] The TOPEX/Scatterometer collocation data set is divided into 10 sub-data sets according to σ_C, as indicated in Table 2. Each sub-data set is then used to determine a specific pair of a_i and b_i by minimizing the summed squares of the altimeter estimated and scatterometer measured wind speed differences, yielding

$$a_i = \frac{N_i \sum_{j=1}^{N_i} \sigma_{Ku}^{i,j} \cdot U_S^{i,j} - \sum_{j=1}^{N_i} \sigma_{Ku}^{i,j} \cdot \sum_{j=1}^{N_i} U_S^{i,j}}{N_i \sum_{j=1}^{N_i} \left(\sigma_{Ku}^{i,j}\right)^2 - \left(\sum_{j=1}^{N_i} \sigma_{Ku}^{i,j}\right)^2} \quad (i = 1, 2, \cdots, n) \tag{4a}$$

$$b_i = \frac{\sum_{j=1}^{N_i} \left(\sigma_{Ku}^{i,j}\right)^2 \cdot \sum_{j=1}^{N_i} U_S^{i,j} - \sum_{j=1}^{N_i} \sigma_{Ku}^{i,j} \cdot U_S^{i,j} \cdot \sum_{j=1}^{N_i} \sigma_{Ku}^{i,j}}{N_i \sum_{j=1}^{N_i} \left(\sigma_{Ku}^{i,j}\right)^2 - \left(\sum_{j=1}^{N_i} \sigma_{Ku}^{i,j}\right)^2} \quad (i = 1, 2, \cdots, n) \tag{4b}$$

where U_s is the scatterometer wind speed, and N_i is the number of collocated measurements for the ith sub-data set. The resulting coefficients are given in Table 3, and a graphic illustration of the linear composite model function is presented in Figure 4 (the straight lines labeled 1 through A). The modified Chelton and Wentz (abbreviated as MCW) algorithm [*Witter and Chelton*, 1991] is also superimposed (in red) on Figure 4 for reference. As can be seen, the LCM algorithm appears as a set of straight lines with a gradually decreasing slope. An immediate impression is that such an algorithm is expected to have a much larger degree of freedom for accommodating the generally smooth yet highly nonlinear U–σ_{Ku} relationship. The MCW algorithm is close to the LCM-4 for wind speed higher than 10 m/s (Figure 4). For low winds under 5 m/s, the two algorithms differ considerably: The inferred speed approaches to zero with σ_{Ku} much faster for the MCW model compared to the LCM model. In the medium range of wind speed between 5–10 m/s, the two algorithms overlap as the slope of the LCM changes continuously. One has to be reminded, however, each line of the LCM algorithm is not supposed to be valid for its full range. The portion of which the validity is held can be practically determined according to σ_C.

Table 3. Coefficients of the LCM Wind Speed Algorithm for TOPEX Proposed in This Study

Group Index (i)	a_i	b_i
1	−4.625561039	56.60987665
2	−4.112881436	51.43683222
3	−3.683242160	48.17670139
4	−3.177943303	43.32457803
5	−2.316302887	33.36103571
6	−1.393144971	21.82045494
7	−0.813285207	14.18267245
8	−0.583828302	10.92756962
9	−0.372227324	7.873853105
A	−0.252240602	6.012448072

4. Validation and Intercomparison

[13] In this section, the LCM model function will be validated against global buoy data, and intercompared using ECMWF winds. In doing so, two other altimeter wind speed algorithms, i.e., the *Witter and Chelton* [1991] (MCW), and the *Gourrion et al.* [2002] (denoted as G02), are also employed for comparisons. These two algorithms are selected because the former has been in operational use for past and ongoing altimeter missions, and the latter is concluded by *Gommenginger et al.* [2002], following a systematic validation, to have the best overall performance compared to *Witter and Chelton* [1991], *Glazman and Greysukh* [1993], and *Freilich and Challenor* [1994].

4.1. Validation Against Buoy Data

[14] Traditionally, buoy data are considered as the best available sea truths for satellite algorithm validation. The 4512 coincident TOPEX/Buoy winds used here cover a time period from September 1992 to December 1998, and a latitude band between 17.2°N and 59.3°N (see Table 1). Given its large quantity, long duration and wide spatial coverage, this data set is believed to be "good enough" for validation purposes. An important characteristic for a useful algorithm is that the derived wind speed histogram respects the shape of the reference wind speed distribution. Figure 5 shows the wind speed histograms obtained from the buoy measurements (black), as well as the altimeter estimates based on the LCM (red), the MCW (green) and the G02 (blue) algorithms. It can be seen that the LCM algorithm produces a histogram which best resembles the sea true. The MCW result agrees well with the buoy result for wind speed

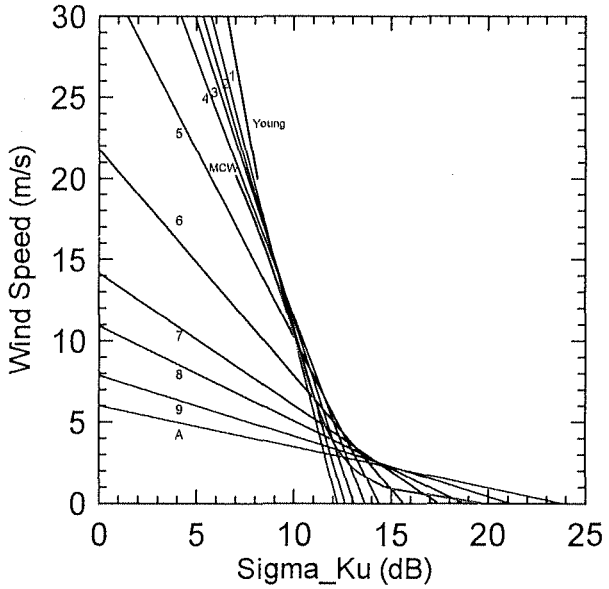

Figure 4. The straight lines labeled 1 through A are the graphic illustration of the LCM wind speed algorithm (see Table 3) developed for TOPEX in this study. Also overlaid are the MCW (in red) and *Young* [1993] (in blue) algorithms.

above 7 m/s, but for low wind speed a considerable distortion can be found. The G02 histogram exhibits the largest departure from other three. It favors strongly on the medium wind speed around 7 m/s while displays a systematically lower probability for both high and low winds.

[15] Next, following the common practice, the mean bias and RMS difference of TOPEX and buoy winds with respect to a reference wind for the three algorithms concerned are presented in Figure 6. The reference wind is defined as the mean value of the buoy and three altimeter wind estimates from the MCW, G02, and LCM algorithms. The reason that this reference wind speed is used for plotting Figure 6 instead of the buoy wind itself is to avoid the artifact of abnormal statistics at low winds caused by the binning [*Freilich*, 1997; *Wentz and Smith*, 1999]. Note that this reference wind speed is used for visualization purposes only, i.e., for the plotting of Figure 6 (and Figure 8 below), all the quantitative statistics summarized in Table 4 are computed against the true buoy or ECMWF winds, respectively. It is evident from Table 4 that the improvement of our algorithm compared to the two others is significant:

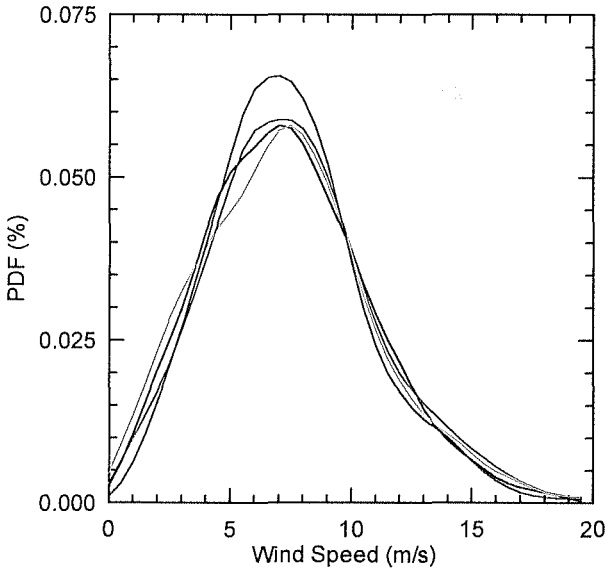

Figure 5. Wind speed histogram based on the TOPEX/Buoy collocation data set. The black, red, green, and blue curves are obtained from the buoy measurement and the altimeter estimates based on the LCM, MCW, and G02 algorithm, respectively.

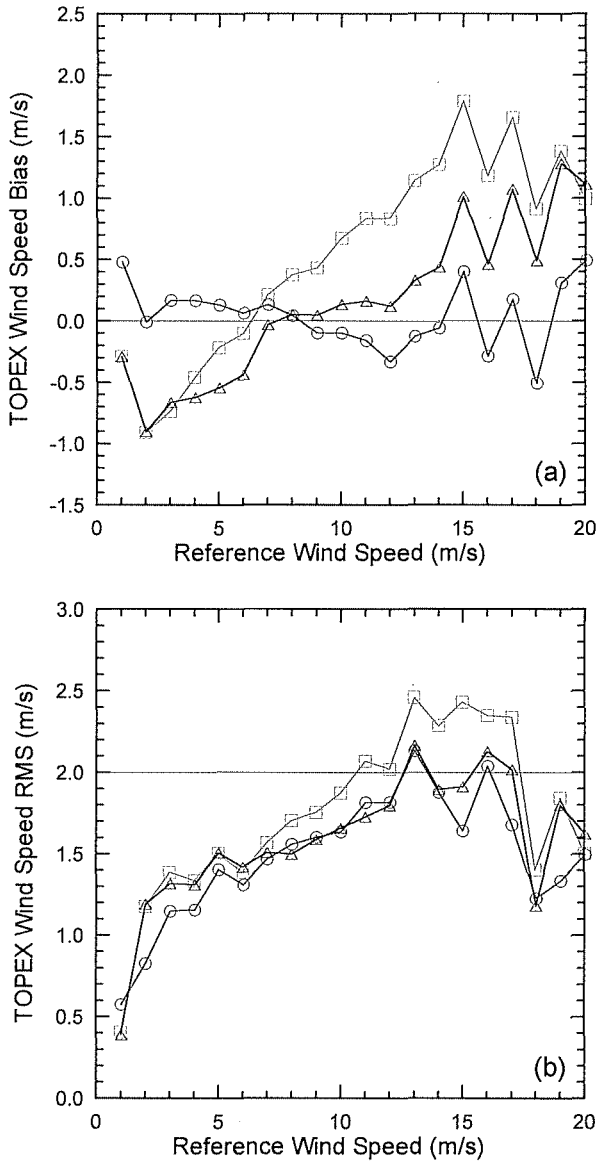

Figure 6. (a) Bias and (b) RMS of TOPEX versus buoy winds with respect to a reference wind speed (see text for more details). The green curve with squares, blue curve with triangles, and red curve with circles correspond to the MCW, G02, and LCM algorithm, respectively. The thin black line indicates a zero bias in Figure 6a and a 2 m/s RMS in Figure 6b.

Table 4. Summary of Comparison Statistics of the MCW, G02, and LCM Altimeter Wind Speed Algorithms

	Bias, m/s			RMS, m/s		
	MCW	G02	LCM	MCW	G02	LCM
Buoy	0.36	−0.05	0.00	1.77	1.60	1.56
ECMWF	0.39	−0.20	−0.04	1.84	1.76	1.65

0.00 m/s (LCM) versus 0.36 m/s (MCW) and −0.05 m/s (G02) in terms of mean bias, and 1.56 m/s (LCM) versus 1.77 m/s (MCW) and 1.60 m/s (G02) in terms of overall RMS. Figure 6a shows that the bias of the LCM algorithm fluctuates within a narrow band between ±0.5 m/s for most of the wind speeds. The amplitude of the MCW and G02 biases is seen to be much larger. Moreover, both the MCW and the G02 algorithms seem to underestimate the wind speed at low winds while overestimate it at high winds. As far as the RMS error is concerned, our result is systematically lower than the MCW result for almost the entire range of wind speed under consideration (Figure 6b). The LCM and G02 algorithms are very close to each other for moderate speeds between 7–14 m/s, but the LCM algorithm is seen to have a generally better performance for low and high winds beyond that range. This confirms an earlier observation that an H_s dependent algorithm is most likely to be effective for medium winds where the U–H_s dependency is better defined (see Figure 3a), provided it has large

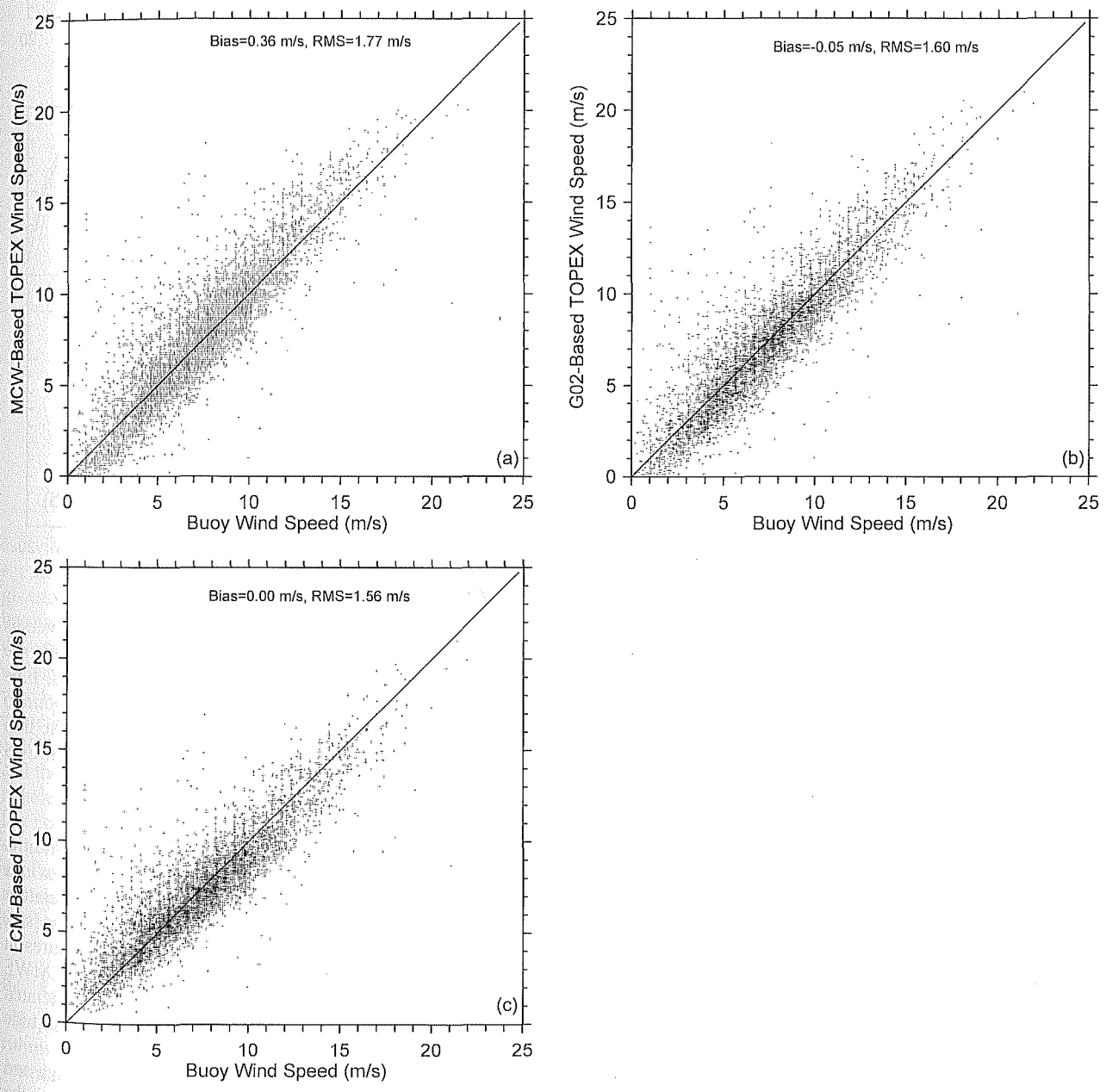

Figure 7. Scatter diagrams of TOPEX versus buoy wind speeds. The (a) MCW, (b) G02, and (c) LCM algorithms are used for deriving TOPEX wind speed. A perfect line is also overlaid on each subplot.

enough degrees of freedom (note that there are 15 coefficients in the G02 algorithm).

[16] The scatter diagrams of the MCW, G02 and LCM derived wind speeds with respect to the buoy winds are plotted in Figures 7a, 7b and 7c, respectively. A perfect line is also overlaid on each subplot. Apparently, the MCW result (Figure 7a) has the largest spreading among the three. Both the G02 (Figure 7b) and the LCM (Figure 7c) results are well balanced with respect to the perfect line, with the latter being slightly more concentrated for low and high winds. Figure 7 provides a visual confirmation that a significantly higher accuracy of wind speed estimate has been achieved by both the LCM and the G02 algorithms.

[17] It should be mentioned that a direct validation of the LCM algorithm for wind speed above 20 m/s is not conducted in the present study for two reasons. First, there are not enough coincident high winds in our collocation data set to allow a statistically significant comparison. Second, wind speed beyond 20.154 m/s is not available from the MCW algorithm [*Witter and Chelton*, 1991]. However, an indirect check can be made based on an algorithm developed specifically for high wind speed between 20 m/s and 40 m/s [*Young*, 1993]. In doing so, part of Young's linear model function is superimposed (in blue) on Figure 4. It is found that the trend of Young's model converges nicely with our model at the high end. The observed smooth transition serves as evidence that the LCM algorithm is able to produce reasonable wind estimates up to a given limit beyond 20 m/s.

4.2. Intercomparison Using ECMWF Winds

[18] Based on the above validation, it is already clear that the quality of TOPEX wind speed estimate can be considerably enhanced by applying the LCM approach. This will be further confirmed by an intercomparison using another independent data set, the ECMWF winds. Figure 8 is the same kind of plot as Figure 6, except that the buoy data are replaced by the ECMWF data. This time the degree of improvement is somewhat more obvious: The LCM algorithm has the smallest overall fluctuation in mean bias and a systematically lower RMS for wind speeds below 15 m/s compared to the other two algorithms. For wind speeds higher than 15 m/s, the MCW model produces the smallest RMS among the three. One has to bear in mind, however, when the error of an altimeter wind speed algorithm is concerned, more weights should be given to the intermediates between 5 m/s and 12 m/s where the actual wind measurements are heavily populated. Therefore, the range within which the LCM algorithm has a better performance is wide enough to ensure an overall improvement.

[19] It would be interesting to examine the geographical distribution of the RMS difference of the three wind speed algorithms (Figure 9). The general pattern of the three subplots looks rather similar. The decreasing order of the RMS amplitude, namely $RMS_{MCW} > RMS_{G02} > RMS_{LCM}$ as indicated by their overall RMS (1.84 m/s, 1.76 m/s and 1.65 m/s, see Table 4), is held for almost everywhere in the ocean. For all three subplots, relatively low RMS values are found in the tropical oceans. The uncertainty increases poleward with latitude. Large RMSs are observed in the Pacific and Indian Ocean sectors of the Southern Ocean, as well as in the North Pacific and Northwest Atlantic. Although large errors are mostly associated with high winds in Figure 9, there is not a clear geographical correlation between the distributions of RMS and wind intensity [see, e.g., *Chen et al.*, 2002b, Figure 1]. The regional features in Figure 9 are most likely to be a reflection of the ECMWF model deficiency, while the varying uncertainties associated with the altimeter algorithms tend to modulate the amplitude of these features.

[20] In summary, validation against global buoy data and intercomparison using ECMWF winds both suggest that the improvement of the LCM algorithm is substantial over the MCW algorithm, and is significant over the G02 algorithm,

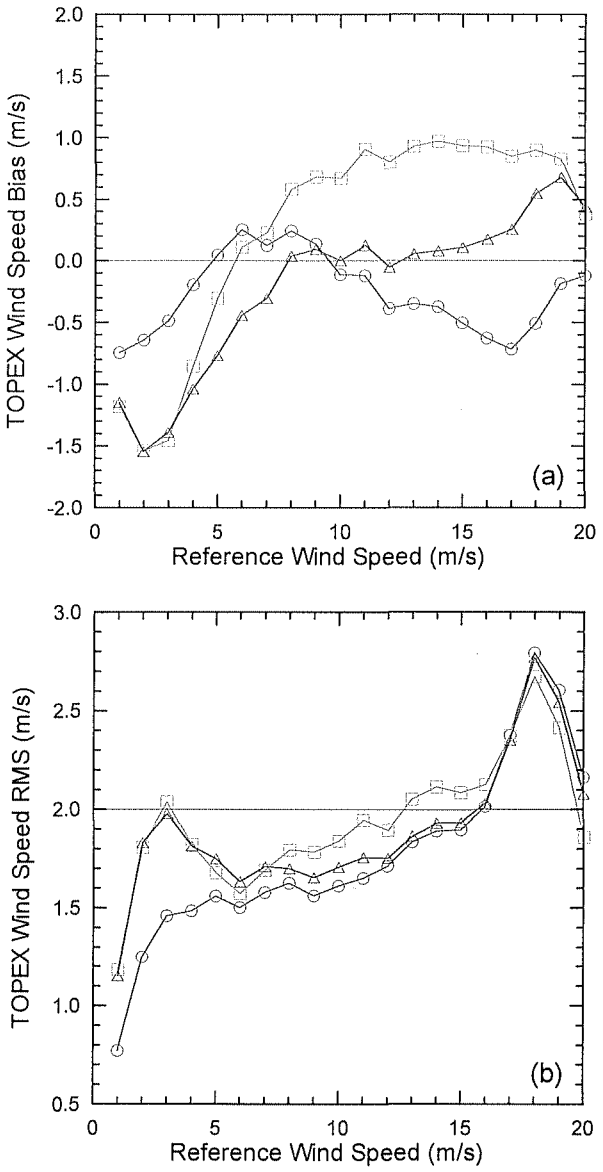

Figure 8. (a) Bias and (b) RMS of TOPEX versus ECMWF winds with respect to a reference wind speed (see text for more details). The green curve with squares, blue curve with triangles, and red curve with circles correspond to the MCW, G02, and LCM algorithm, respectively. The thin black line indicates a zero bias in Figure 8a and a 2 m/s RMS in Figure 8b.

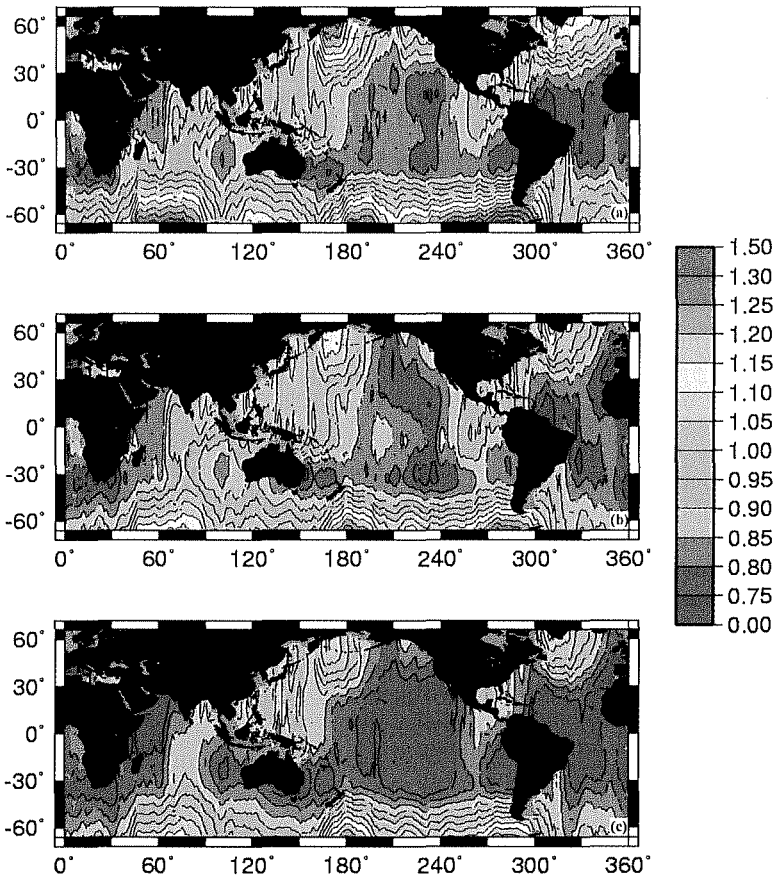

Figure 9. Geographical distributions of the RMS difference between the TOPEX and the ECMWF wind speeds. The (a) MCW, (b) G02, and (c) LCM algorithms are used for deriving TOPEX wind. The color scale is in m/s.

as evidenced in Figures 5–9 and quantified in Table 4. It should be pointed out that algorithm evaluation statistics given by various authors are, in most cases, incomparable because of the different reference data used and the different data editing criteria applied. For example, removal of the outliers whose wind speed difference is greater than 5 m/s with respect to the reference data may lead to a considerable reduction of 10–20% in overall RMS (in the case of our TOPEX/Buoy collocation data, the reduction is about 16%, and the overall RMS of the MCW, G02 and LCM algorithm reduces to 1.49, 1.35 and 1.31 m/s, respectively). But this has nothing to do with the algorithm performance and may sometimes result in misleading conclusions when compared to other validation statistics. In our analysis, all original data are used except those with abnormal quality flags, in order to obtain a more realistic assessment.

5. Concluding Remarks

[21] More than a dozen of altimeter wind speed algorithms have been developed over the past twenty years as a continuing effort to improve the accuracy from a sensor designed value of 2 m/s toward a somewhat geophysically satisfactory value of 1 m/s. Given the 0.8 m/s error budget of buoy wind measurement [*Gilhousen*, 1987], which is widely used as sea truth in algorithm validation, the level of 1 m/s can perhaps be considered as the full potential of wind speed estimate by altimeters of the present generation. As regrettably admitted by some investigators [e.g., *Hwang et al.*, 1998], however, real progress in wind speed retrieval remains stagnant for the past decade despite of the continuous improvement of the altimeter hardware and software. The two kinds of available algorithms, namely, theoretical and empirical, each faces its own constraint. Theoretical analysis has clearly suggested that a single satellite instrument, such as the altimeter or the scatterometer, is intrinsically incapable of unambiguously measuring the wind speed under a wide range of sea state [e.g., *Glazman and Pilorz*, 1990]. Knowing the prevalence and complexity of swell/wind sea coupling in the actual ocean [e.g., *Chen et al.*, 2002a], purely theoretical model functions have little chance to reach the expected accuracy in their present forms. On the other hand, it is the authors' view that the performance of many current empirical algorithms is considerably limited by the low degree of freedom (represented by the number of independent variables and model coefficients) due to the predescribed forms of the model functions. It is believed that, in the foreseeable future, a more realistic hope of achieving the 1 m/s accuracy will have to rely on empirical (or semitheoretical) algorithms

with larger degrees of freedom provided by the increasing volume of high quality validation data, and additional independent measurements such as σ_C.

[22] As a pioneering work of its kind, a linear composite wind speed algorithm for TOPEX altimetry is proposed in this study. Validation of our algorithm against the MCW and G02 model functions using an extensive buoy data set indicates an improvement in overall RMS of 12% and 2.5%, respectively (Table 4). The effectiveness and efficiency of the LCM approach are further demonstrated on both global and regional scales via an algorithm intercomparison based on ECMWF winds. The RMS reduction of the LCM for this data set is 10% and 6% compared to the MCW and G02, respectively (Table 4). In addition to its high accuracy under a wide range of wind speed (in contrast to several previous algorithms whose improvement is limited to a given band), a unique advantage of the LCM scheme is its unprecedented flexibility in model refinement. The elegant linear nature allows it to be easily adjusted or expanded within a given range of wind speed without affecting the rest. An immediate example is that the *Young* [1993] algorithm can be directly integrated into our model function as an expansion. Such flexibility is particularly attractive for the development of regional or seasonal wind algorithms. To conclude, we would like to emphasize that the potential of the LCM scheme in further advancing altimeter wind speed estimate is perhaps more important than the present algorithm itself, though it is believed that the LCM model function in its present form is already a good candidate to compete for operational use.

[23] Finally, it should be pointed out that despite of the recent richness and growing success of scatterometer satellites, wind products derived from other spaceborne sensors will continue to prove their usefulness and, in some cases, play their unique roles in the future. As far as the altimeter wind is concerned, this can be understood for the following reasons. First, the spatial and temporal sampling of current scatterometers is far from ideal for tracking the evolution of many important local/regional transient events such as storms. Extra coverage in space or time is always desirable provided the same level of wind speed accuracy is reached. Second, the retrievals of wind speeds from scatterometers and altimeters are based on different physical backgrounds: Bragg resonant scattering for the former, while specular reflection for the latter. This may lead to a complementary nature for the qualities of the two types of products in terms of systematic errors. Third, the altimeter wind has a number of unique advantages. For example, the capability of providing exactly simultaneous wind/wave measurements makes it very useful in the studies of wave growth and air-sea interaction. In addition, contrary to scatterometers, the non-Sun synchronous orbit of altimeter satellite makes it possible to study the diurnal variation of wind speed over the ocean, in particular the land breeze and sea breeze phenomena. It is therefore obvious that altimeters will continue to make significant contributions to global oceanic wind observation for many years to come.

[24] **Acknowledgments.** This work is cosponsored by the Natural Science Foundation of China (projects 40025615 and 40271083), the National High Technology Program of China (project 2001-AA63-0306), and the Teaching and Research Award Program for Outstanding Young Teachers in Higher Education Institutions of MOE, PRC. The authors are very grateful to C. P. Gommenginger at the Southampton Oceanography Center, who kindly provided the TOPEX/Buoy collocation data set.

References

Brown, G. S., H. R. Stanley, and N. A. Roy, The wind speed measurement capability of spaceborne radar altimeters, *IEEE J. Oceanic Eng.*, *6*, 59–63, 1981.

Chen, G., B. Chapron, J. Tournadre, K. Katsaros, and D. Vandemark, Global oceanic precipitation: A joint view by TOPEX and the TOPEX microwave radiometer, *J. Geophys. Res.*, *102*, 10,457–10,471, 1997.

Chen, G., B. Chapron, R. Ezraty, and D. Vandemark, A global view of swell and wind sea climate in the ocean by satellite altimeter and scatterometer, *J. Atmos. Oceanic Technol.*, *19*, 1849–1859, 2002a.

Chen, G., R. Ezraty, C. Fang, and L. Fang, A new look at the zonal pattern of the marine wind system from TOPEX measurements, *Remote Sens. Environ.*, *79*, 15–22, 2002b.

Elfouhaily, T., D. Vandemark, J. Gourrion, and B. Chapron, Estimation of wind stress using dual-frequency TOPEX data, *J. Geophys. Res.*, *103*, 25,101–25,108, 1998.

Freilich, M. H., Validation of vector magnitude data sets: Effects of random component errors, *J. Atmos. Oceanic Technol.*, *14*, 695–703, 1997.

Freilich, M. H., and P. G. Challenor, A new approach for determining fully empirical altimeter wind speed model functions, *J. Geophys. Res.*, *99*, 25,051–25,062, 1994.

Freilich, M. H., and R. S. Dunbar, The accuracy of the NSCAT 1 vector winds: Comparisons with National Data Buoy Center buoys, *J. Geophys. Res.*, *104*, 11,231–11,246, 1999.

Gilhousen, D. B., A field evaluation of NDBC moored buoy winds, *J. Atmos. Oceanic Technol.*, *4*, 94–104, 1987.

Glazman, R. E., and A. Greysukh, Satellite altimeter measurements of surface wind, *J. Geophys. Res.*, *98*, 2475–2483, 1993.

Glazman, R. E., and S. H. Pilorz, Effects of sea maturity on satellite altimeter measurements, *J. Geophys. Res.*, *95*, 2857–2870, 1990.

Gommenginger, C. P., M. A. Srokosz, P. G. Challenor, and P. D. Cotton, Development and validation of altimeter wind speed algorithms using an extended collocated buoy/TOPEX data set, *IEEE Trans. Geosci. Remote Sens.*, *40*, 251–260, 2002.

Gourrion, J., D. Vandemark, S. Bailey, B. Chapron, C. P. Gommenginger, P. G. Challenor, and M. A. Srokosz, A two parameter wind speed algorithm for Ku-band altimeters, *J. Atmos. Oceanic Technol.*, *19*, 2030–2048, 2002.

Hwang, P. A., W. J. Teague, G. A. Jacobs, and D. W. Wang, A statistical comparison of wind speed, wave height, and wave period from satellite altimeters and ocean buoys in the Gulf of Mexico region, *J. Geophys. Res.*, *103*, 10,451–10,468, 1998.

Lefevre, J. M., J. Barckicke, and Y. Ménard, A significant wave height dependent function for TOPEX/Poseidon wind speed retrieval, *J. Geophys. Res.*, *99*, 25,035–25,049, 1994.

Quartly, G. D., M. A. Srokosz, and T. H. Guymer, Global precipitation statistics from dual-frequency TOPEX altimetry, *J. Geophys. Res.*, *104*, 31,489–31,516, 1999.

Queffeulou, P., B. Chapron, and A. Bentamy, Comparing Ku band NSCAT scatterometer and ERS-2 altimeter winds, *IEEE Trans. Geosci. Remote Sens.*, *37*, 1662–1670, 1999.

Wentz, F. J., and D. K. Smith, A model function for the ocean-normalized radar cross section at 14 GHz derived from NSCAT observations, *J. Geophys. Res.*, *104*, 11,499–11,514, 1999.

Witter, D. L., and D. B. Chelton, A Geosat altimeter wind speed algorithm and a method for altimeter wind speed algorithm development, *J. Geophys. Res.*, *96*, 8853–8860, 1991.

Wu, J., On wave dependency of altimeter sea returns-Weak fetch influence on short ocean waves, *J. Atmos. Oceanic Technol.*, *16*, 373–378, 1999.

Young, I. R., An estimate of the Geosat altimeter wind speed algorithm at high wind speeds, *J. Geophys. Res.*, *98*, 20,275–20,285, 1993.

B. Chapron and R. Ezraty, Département d'Océanographie Physique et Spatiale, Centre de Brest, IFREMER, B. P. 70, 29280 Plouzané, France.

G. Chen, Ocean Remote Sensing Institute, Ocean University of China, 5 Yushan Road, Qingdao 266003, China. (gcchen@public.qd.sd.cn)

D. Vandemark, Laboratory for Hydrospheric Processes, Wallops Flight Facility, NASA Goddard Space Flight Center, Code 972, Building 159, Wallops Island, VA 23337, USA.